

ORIGINAL ARTICLE

Antifungal Activity of Biologically Synthesized Metallic Nanoparticles from *Streptomyces* species SS7

Areej M. El-Mahdy*, Mona Shaaban

Department of Microbiology and Immunology, Faculty of Pharmacy, Mansoura University, Mansoura 35516, Egypt

ABSTRACT**Key words:**

Nanoparticles,
Streptomyces, 16S rRNA
sequence analysis,
Phylogenetic relationship,
Antifungal activity

***Corresponding Author:**

Areej M. El-Mahdy,
Department of Microbiology
and Immunology, Faculty of
Pharmacy, Mansoura
University, Mansoura 35516,
Egypt,
Tel.: 01224212473
areej@mans.edu.eg;
areej_243@yahoo.com

Background: One area of nanotechnology that has transformed the biological sciences is green manufacturing of nanoparticles. **Objectives:** This work aims to report the antifungal activities of selenium (Se) and silver (Ag) nanoparticles (NPs) from *Streptomyces* SS7 using an environmentally safe technique. **Methodology:** Identification of *Streptomyces* SS7 using 16S rRNA sequence analysis was done and synthesis of Se and AgNPs was examined by ultraviolet–visible spectroscopy, transmission electron microscopy (TEM), and dynamic light scattering (DLS). The antifungal activity of NPs against *Candida albicans* and *Aspergillus fumigatus* was assessed. **Results:** Based on 16S rRNA sequence, *Streptomyces* SS7 was linked to *Streptomyces sporocinereus*, *Streptomyces hygroscopicus*, *Streptomyces endus* and *Streptomyces demainii*. Absorption bands of Se and AgNPs were obtained around 230 and 250 nm. TEM showed spherical particles with size range from 11–24 nm. SeNPs measured 2.93 and 101.8 nm in size, while AgNPs measured 9.432 nm using DLS. MICs of AgNPs were 1.25 mg/mL against *Candida* and less than 0.075 mg/mL against *Aspergillus fumigatus*. *Candida albicans* and *Aspergillus fumigatus* had MICs of 2.5 mg/mL for SeNPs except for *Candida albicans* C12 and *Candida albicans* CA, were 1.25 and 5 mg/mL. **Conclusion:** this study demonstrated the fungistatic activity of Se and AgNPs with a higher potency of AgNPs.

INTRODUCTION

Severe fungal infections have recently been linked to a considerable rise in the morbidity and mortality of patients with impaired immune systems requiring intensive care encompassing the administration of broad-spectrum antibiotics¹⁻². *Candida* spp. are among the most common organisms that cause fungal infections, which can have a death rate of up to 40%.³. Nowadays, the majority of accessible and efficacious antifungal medicines are derived from polyenes, triazoles, or echinocandins. Nevertheless, using these antifungals often leads to a variety of negative effects, such as azole toxicity, amphotericin B toxicity, and yeast resistance to antifungal therapy⁴⁻⁵. Therefore, alternative approaches to efficacious antifungal medication are needed to prevent the aforementioned side effects.

Nanoparticles have attracted a lot of attention recently for a variety of fields of life, from industrial to health care, due to possession of several distinct physical and chemical characteristics that make them different from their counterparts in bulk materials. These materials have been embraced and applied in the fields of medicine, the environment, and agriculture⁶. Nanomaterials with demonstrated efficacy in managing various ailments include metallic oxides, nonmetals, carbon nanomaterials, and metallic oxides⁷. Biological techniques for green nanosynthetic methods are

generally economical, environmentally safe, and time-efficient, so they yield notable outcomes for nanotechnology. Metal reduction through particular metabolic pathways of different organisms has been determined as a possible source of nanoparticles production⁸.

Streptomyces is a genus of Gram-positive aerobic bacteria that may thrive in diverse conditions. Their filamentous shape resembles that of fungus⁹. *Streptomyces* organisms are widely employed in the enzyme, pharmaceutical, and agricultural sectors because they generate potent bioactive chemicals. They are therefore well-known for their industrial manufacturing capabilities¹⁰.

This research investigated the reduction capability of *Streptomyces* spp. (SS7) isolated from beaches for the production of selenium (Se) and silver (Ag) nanoparticles (NPs). Properties of the synthesized nanoparticles were then investigated using ultraviolet–visible (UV–vis), transmission electron microscopy (TEM), and particle size analysis. Also, the produced NPs were tested for their antifungal activities.

METHODOLOGY**Isolation and molecular identification of *Streptomyces***

Fifteen Soil samples were taken from different beaches of Alexandria, Damietta, and Gamasa,

processed for isolation and purification of streptomycetes. Soil sample were processed using Shaaban and El-Mahdy's methodology¹¹. ISP-2 medium was employed to isolate the streptomycetes strains¹². Only one streptomycetes isolate was chosen to synthesize the Se and Ag NPs.

The molecular characterization of streptomycetes isolate SS7 was performed through the 16S rRNA method¹³. Genomic DNA of the isolate SS7 was extracted according to¹⁴. The 16S rRNA was amplified and sequenced using primers forward: 5'-AGAGTTTGATCMTGGCTCAG-3' and reverse: 5'-ACGAGCTGACGACARCCATG-3' (ABI 3730xl sequencer, Applied Biosystems). Sequences of related species were obtained by resolving nucleotide sequences using the National Centre for Biotechnology Information's (NCBI) basic local alignment search tool. Using Molecular Evolutionary Genetics Analysis (MEGA) Version 5.0¹⁵ and the neighbour-joining method¹⁶, sequence alignments were carried out, and a phylogenetic tree was created.

Cultural characters of streptomycetes isolate SS7

Cultural characteristics of *Streptomyces* SS7 were investigated; including spores color, diffusible pigment, and melanin production¹⁷. Using a technique outlined by Zonaro et al.¹⁸, scanning electron microscopy (JEOL JSM 6510 lv) was used to investigate the spore chain morphology of SS7.

Biological synthesis of Se, and Ag NPs

Synthesis of Se and Ag NPs was performed using the procedure described by¹⁹. *Streptomyces* SS7 was cultured in 50 ml ISP-2 media incubated at 28°C for 3 days with agitation at 150 rpm. A 10-minute centrifugation at 10,000 rpm was then applied to the culture and the harvested mycelial mass was 2.5 mg/ml (wet weight). The cell-free extract was mixed with solutions of SeO₂ and AgNO₃ until a final concentration of 5 mM was achieved. A control flask (without SeO₂, AgNO₃) was also used. Samples were taken for the purpose of characterizing the produced nanoparticles (NPs) using visible colour changes of the cell-free extracts at 24, 48, and 72 hours.

Characterization of Se and Ag NPs

A UV-Vis spectrophotometer 1601 pc in the range from 200 to 700 nm at a resolution of 1 nm was used to assess the absorption spectral bands of the biologically synthesised Se and Ag NPs. The control solution (media treated only with SeO₂, and AgNO₃) was used²⁰.

Using TEM (JEOL JEM-2100, UK), the micrograph of the synthesised Se and Ag NPs was analyzed to

ascertain the morphology and dispersion of the produced NPs²¹.

A particle size analyzer and the dynamic light scattering (DLS) technique with laser light (Microtrac, nanotrak wave II Q) were used to measure the particle size distribution.

Antifungal activity of the synthesised NPs

The antifungal activity of both Se and Ag NPs was evaluated using the microbroth dilution²² against 7 strains of *Candida albicans* isolated from vaginal swabs, and one strain of *Aspergillus fumigatus* (Af293) by using 2-fold serial dilutions of Se and Ag NPs (5 – 0.075 mg/mL) and the results were compared with the antifungal drug fluconazole (standard). Sterile saline containing 1% Tween 80 was used to prepare stock solutions from colonies that were 7 days old and cultivated on Sabouraud dextrose agar plates. Cultures were adjusted to the turbidity equivalent to 0.5 McFarland standard (10⁸ CFU/ml) prepared from a fresh subculture in Sabouraud Dextrose Broth (SDB), then the suspension was diluted to 10⁶ CFU/ml. The adjusted microbial inoculums (100 µl) were added to each well of sterile flat-bottomed 96-well microtiter plate containing the tested concentration of Se, and AgNPs (100 µl/well). Upon incubation for 36 hours at 37°C, the minimum inhibitory concentration (MIC) was determined to be the lowest value that prevented the observable growth of bacteria.

Statistical analysis

Every experiment was run three times, and the mean of the data was calculated using Excel spreadsheet. The formed Se and Ag NPs' MICs were compared to the control antifungal fluconazole's MIC using the paired t test; findings were regarded significant when P < 0.05.

RESULTS

Isolation, cultural characters and molecular identification of Streptomyces

Fifteen soil samples were obtained from different beaches of Alexandria, Damietta, and Gamasa. The isolate that was selected to complete this study is an aerobic filamentous Gram-positive bacterium with wrinkled, rugose colonies, producing white mycelia that turned grey after 21 days of incubation at 28°C. No production of melanin pigments was observed. The SEM showed that the aerial mycelia produce spiral spore chains. The spore surface was rugose (Figure 1).

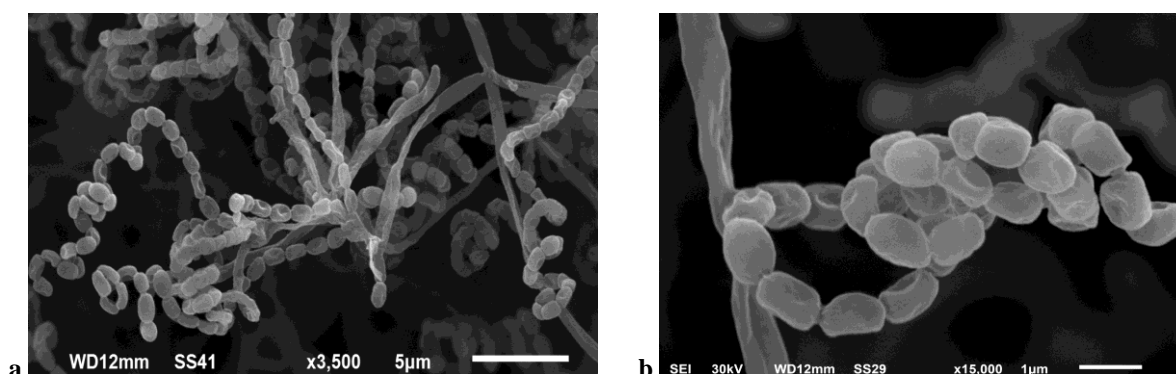


Fig. 1: Scanning electron micrograph of spore chain morphology of *Streptomyces* sp. SS7

The impact of heavy metals on the growth of *Streptomyces* isolate was investigated using ISP-2 medium supplemented with SeO₂ and AgNO₃ at concentrations ranging from 1 to 10 mM. The isolate SS7's whole 16S rRNA gene sequence was identified in this work and submitted to GenBank with the accession number PP410316. The sequencing analysis stipulated that SS7 is a member of the *Streptomyces* genus. Using the neighbour-joining method, the phylogenetic tree was constructed¹⁶. Figure 2 displays the isolate SS7's

location in relation to the streptomyces type strains. The findings obtained from the 16S rRNA gene analysis and phylogenetic tree revealed that strain SS7 is related to *Streptomyces sporocinereus* strain NBRC 100766 (NR_041412.1), *Streptomyces hygroscopicus* strain NBRC 13472 (NR_041145.1), *Streptomyces endus* strain NRRL 2339 (NR_043379.1), and *Streptomyces demainii* strain NRRL B-1478 (NR_043723.1) with a 99.3% similarity.

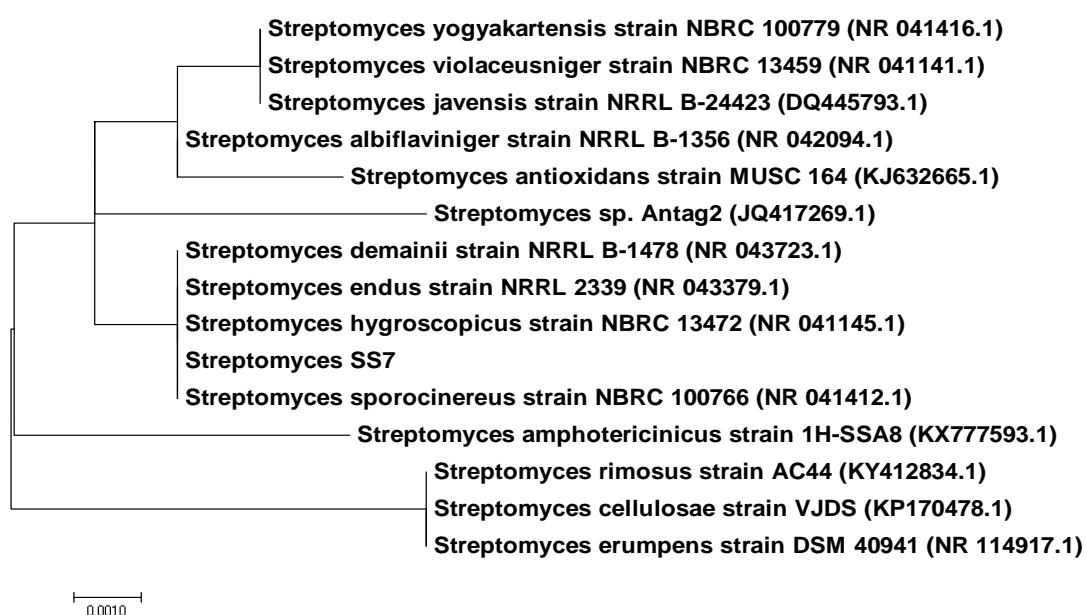


Fig. 2: A neighbour-joining tree based on 16S rRNA gene sequences illustrating the relationship between isolate SS7 and closely related *Streptomyces* species.

Description of the formed NPs

Extracellular microbial generation of both Se and Ag NPs was carried out in the present investigation using the cell-free extract of *Streptomyces* isolate SS7. This was verified by the colour change of the supernatant

into orange and brown colour of the culture treated with the metal ions, whilst the control flask's colour remained unchanged as seen in Figure 3. It was noted that upon incubation, the colour change became more intense with marked deep coloration after 72 h incubation.

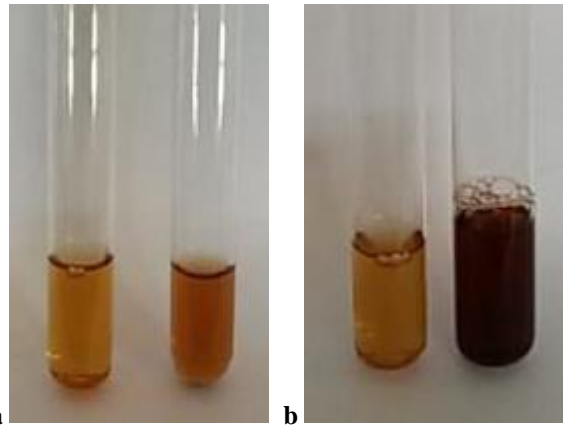


Fig. 3: Colour change of the synthesized NPs using cell-free extract of *Streptomyces* isolate SS7
 (a) Se NPs with orange colour, (b) Ag NPs with brown colour

Using UV-vis spectroscopy, the bioreduction of Se^{4+} , and Ag^+ ions in the cell free supernatant was observed. Figure 4 shows the UV-vis spectra of both SeNPs and AgNPs. AgNPs synthesis increased slightly by time, while the concentration of bio-reduced Se NPs

didn't change. SeNPs displayed a prominent absorption spectral peak at 230 nm (Fig. 4a), while AgNPs showed a surface plasmon resonance band around 250 nm (Fig. 4b).

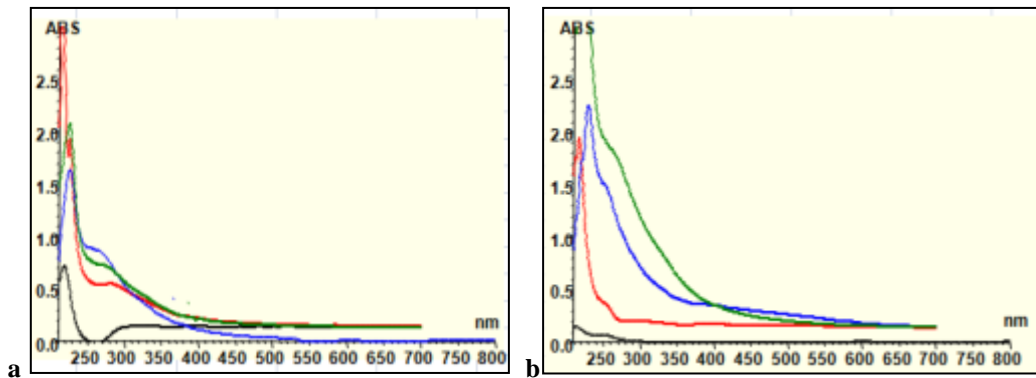


Fig. 4: UV-vis spectra of synthesised NPs by cell-free filtrate of isolate SS7.
 (a) Se NPs, (b) Ag NPs

Ag and Se NPs had a spherical form, and exhibit a size ranging from (11-24 nm) as observed by the TEM images (Figure 5).

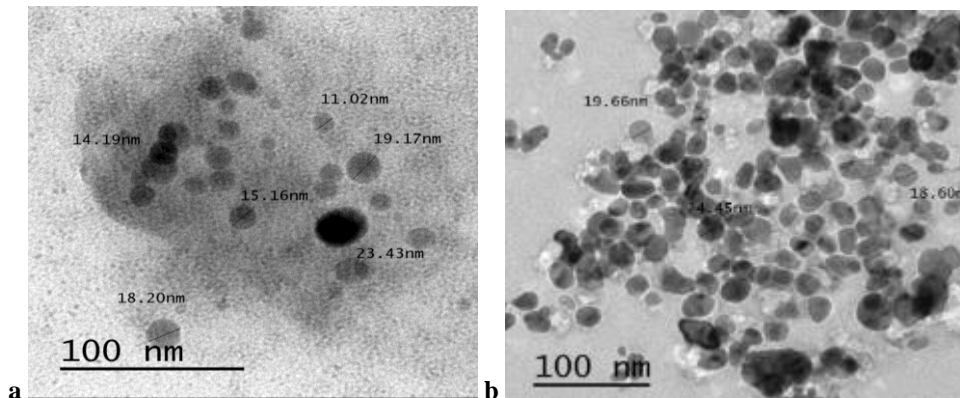


Fig. 5: TEM images of (a) SeNPs, and (b) Ag NPs

Fig. 6 shows the size distribution determined by the laser light scattering method for Se, and Ag NPs. Se NPs' range of particle sizes was 2.93 nm for the first peak and 101.8 nm for the second one that showed

higher frequency as determined by DLS (Fig. 6a). For Ag NPs, one peak was clearly observed at 9.432 nm (Fig. 6b).

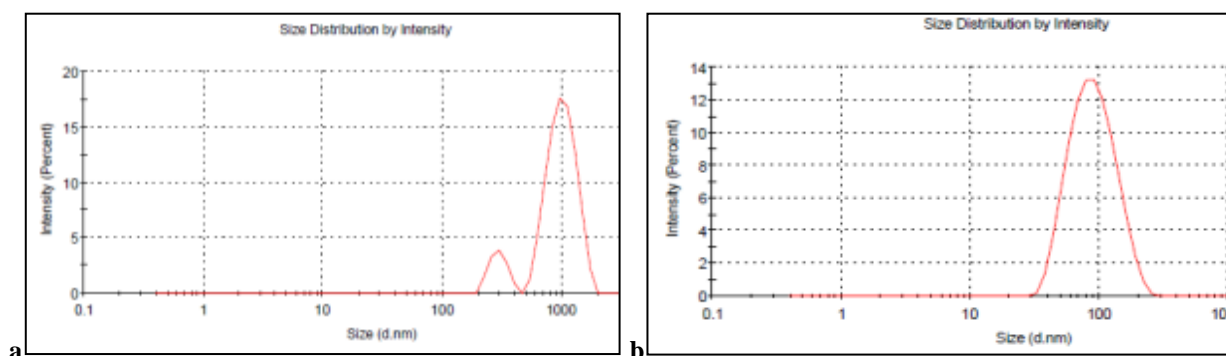


Fig. 6: Particle size distribution for (a) SeNPs and (b) AgNPs

Antifungal action of the synthesised NPs

Table 1 demonstrated that both Se and Ag NPs exhibited antifungal activity against the investigated fungal strains, with Ag NPs exhibiting a stronger fungistatic effect than Se NPs. AgNPs showed MIC values of 1.25 mg/mL for the investigated strains of *Candida* and MIC less than 0.075 mg/mL for

Aspergillus fumigatus (Af293) strain. For SeNPs, MIC values were 2.5 mg/mL for the examined *Candida albicans* and *Aspergillus fumigatus* (Af293) strains except for 2 strains of *Candida albicans* C12 and CA, their MICs were 1.25 and 5 mg/mL respectively, whereas all tested strains exhibited resistance to fluconazole.

Table 1: Antifungal activity of Se and Ag NPs against the tested fungal strains

Organism	SS7 (mg/mL)		Controls (mg/mL)		Antifungal control (mg/mL)
	Se	Ag	Se ₂ O ₃	AgNO ₃	Fluconazole
<i>Candida albicans</i>					
C3	2.5	1.25	> 5	5	> 2
C12	1.25	1.25	> 5	5	> 2
CA	5	1.25	5	0.65	> 2
302	2.5	1.25	2.5	1.25	> 2
305	2.5	1.25	5	0.65	> 2
310	2.5	1.25	5	1.25	> 2
44	2.5	1.25	5	0.65	> 2
<i>Aspergillus fumigatus</i>					
Af293	2.5	< 0.075	5	0.15	> 2

DISCUSSION

The use of actinobacteria such as streptomyces in the biological production of nanoparticles offers a plethora of opportunities for the creation of nanomaterials that could serve as alternative therapeutic agents in several biological fields²³. Biological molecules function as *in vitro* reducing and capping agents by reducing the metal salts and capping the generated nanoparticles. Capping nanoparticles (NPs)

has been shown to avoid agglomeration, decrease toxicity, and enhance antimicrobial efficacy²⁴. Based on this, the current work produced metallic nanoparticles by the streptomyces SS7 bacteria that was selected from fifteen soil samples obtained from different locations of Alexandria, Damietta, and Gamasa beaches. It was noted that upon cultivation on ISP-2 medium²⁵, the isolate produced wrinkled, colonies with white mycelia that turned grey after 3 weeks of incubation at 28°C and absence of melanin pigments production. the spiral

spore chains produced by the aerial mycelia have a rugose surface as examined by SEM. *Streptomyces* isolate SS7 was cultured on ISP-2 medium with concentrations of 1-10 mM of SeO₂ and AgNO₃. No effect on bacterial growth was seen when Se⁴⁺ and Ag⁺ ions were present²⁶.

According to a comparative study of 16S rRNA sequence analysis and phylogenetic tree, results revealed that *Streptomyces* isolate SS7 shares a 99.3% similarity in 16S rRNA gene sequence with *Streptomyces sporocinereus* strain (National Biological Recourse Centre) NBRC 100766, *Streptomyces hygrosopicus* strain NBRC 13472, *Streptomyces endus* strain NRRL 2339, and *Streptomyces demainii* strain (Northern Regional Research Laboratory) NRRL B-1478, as documented by the Kumar et al.²⁷

In this study, Se and Ag NPs were produced from *Streptomyces* isolate SS7. Reduction of both metals was confirmed through visual colour change of cell free supernatants from yellow to orange for SeNPs, and brown colour for AgNPs. Inversely, both SeO₂ and AgNO₃ solution-free controls did not exhibit any colour change. The surface plasmon resonance (SPR) that exists in the biosynthesized Se and Ag NPs could be the cause of this colour shift²⁸. Several methods, including UV-vis spectroscopy, TEM, particle size and zeta potential, were employed to describe the formed NPs. The generated biosynthesized Se and Ag NPs were examined using a UV-Vis spectrophotometer which revealed an absorbance peak of SeNPs at 230 nm. Similarly, the synthesised Se NPs using *K. pneumoniae* and *Pseudomonas alcaliphila* showed UV-vis absorbance bands at 254 nm²⁹⁻³⁰. This results is also closely related to those outlined by Hassan et al.³¹ who observed that the produced SeNPs, which were produced from *Streptomyces parvulus* MAR4, had a pronounced spectral peak at 300 nm. Conversely, unique absorption peaks were seen in the UV-visible spectra of SeNPs extracellularly synthesised by *Pseudomonas aeruginosa*, and *Bacillus cereus* respectively, at 520 and 590 nm³²⁻³³. For AgNPs, the UV-vis spectral analysis showed an absorption peak at 250 nm. This contrasts with findings by Shaaban and El-Mahdy¹¹, who found that Ag had UV-vis absorption spectra around 450 nm and Hashem et al.,³⁴ who revealed a plasmonic peak at 420 nm. It was found that the atomic structure of biosynthesized NPs affects their UV-visible spectra³⁵.

The size, morphology, and dispersion of NPs are factors that affect their biological activity³⁶. The size of NPs and their activity are inversely correlated. This makes an examination of the NPs' morphological characteristics essential. TEM was used to accomplish this goal. The TEM images used in our work showed that Ag and Se NPs had a spherical form and varied in size between 11 and 24 nm. These results were consistent with those of Chi et al.³⁷ who reported the

size of the generated AgNPs ranged from 20.15 – 22.21 nm. In contrast, our findings deviate from those of Hassan et al.³¹, wherein the diameter of SeNPs was observed to vary between 48.8 and 129 nm, despite the TEM micrograph of the particles indicating a spherical form.

The antimicrobial activity of nanoparticles is largely dependent on their particle size. The DLS method was used to assess Se and Ag NPs' size and particle distribution. With regard to SeNPs, the first peak's particle size range was 2.93 nm, while the second peak, which displayed a higher frequency according to DLS, was 101.8 nm. The Lazcano-Ramírez et al. study states that the SeNPs-AGL particle size presents a peak with an average length of 8.08 nm and a peak 2 of 384.3 nm³⁸. For Ag NPs, a peak was clearly observed at 9.432 nm. This was in line with findings published by Singh et al.²¹, who reported that AgNPs made from a different *Streptomyces sp.* have extremely tiny particles (5–50 nm). The size distributions of TEM and DLS exhibits a glaring discrepancy. This could be explained by the fact that, whereas the diameter obtained by DLS indicates the size of a notional sphere that diffuses at the same rate as the particles under study, the diameter recorded by TEM really provided the physical size of the particle.

NPs are a particularly promising strategy for fighting MDR infections³⁹. In this work, the microbroth dilution method was employed to assess the antifungal activity of Se and AgNPs. The studied fungal strains were exposed to both Se and Ag NPs, with Ag NPs demonstrating a more promising antifungal activity than Se NPs, according to the results. AgNPs showed MIC values of 1.25 mg/mL for the investigated strains of *Candida* and less than 0.075 mg/mL for the *Aspergillus fumigatus* (Af293) strain. These results were comparable to those reported by Hashem et al.,³⁴ in which MIC values of AgNPs were 0.0156, 0.125, and 0.0625 mg/mL for *A. flavus*, *A. niger* and for *A. terreus* and *A. fumigatus* respectively. This might be because AgNPs can stick to fungus hyphae and saturate them with solution at higher concentrations, which kills the fungus cells. Ag⁺ is the cause of this inhibitory action, which mostly affects the respiratory chain's enzymes and other membrane-associated enzymes. Ag⁺ may also impact some microbial proteins' expression. Additionally, AgNPs can engage in competitive inhibition with substrates to inactivate the enzymes and prevent them from generating the chemicals required for cellular function. For SeNPs, MIC values were 2.5 mg/mL for the examined *Candida albicans* and *Aspergillus fumigatus* (Af293) strains except for 2 strains of *Candida albicans* C12 and *Candida albicans* CA, their MICs were 1.25 and 5 mg/mL respectively, whereas all tested strains were resistant to the antifungal drug fluconazole. Cell membrane integrity disruption may be a potential goal of SeNPs' antifungal actions by invading the cell membrane. Therefore, a ruptured cell

membrane may allow essential cell components to escape, ultimately causing cell death⁴⁰. Metal nanoparticles (NPs) have been created as antimicrobial agents because of their distinctive properties, which include an increased surface to volume ratio, specific surface area, quantum effects, increased surface reactivity, and unique chemical and physical features⁴¹.

CONCLUSION

Growing interest in green chemistry is due to its affordability, biocompatibility, safety for the environment, and lack of production of hazardous byproducts. The present investigation showed the production of both Se and Ag NPs from *Streptomyces* SS7 isolated from soil of beaches. UV-vis spectroscopy, particle size, and TEM were used to characterize the generated NPs. Promising fungistatic action towards the examined fungal strains was displayed by the isolated *Streptomyces* sp. SS7 Se and Ag NPs.

Declarations:

Consent for publication: Not applicable

Availability of data and material: Data are available upon request.

Competing interests: The author(s) declare no potential conflicts of interest with respect to the research, authorship and/or publication of this article. This manuscript has not been previously published and is not under consideration in another journal.

Funding: Authors did not receive any grants from funding agencies.

REFERENCES

- Pappas PG, Rex JH, Lee J, Hamill RJ, Larsen RA, Powderly W, Kauffman CA, Hyslop N, Mangino JE, Chapman S. A prospective observational study of candidemia: epidemiology, therapy, and influences on mortality in hospitalized adult and pediatric patients. *Clinical Infectious Diseases* 2003, 37 (5), 634-643.
- Pfaller MA, Diekema D. Epidemiology of invasive candidiasis: a persistent public health problem. *Clinical microbiology reviews* 2007, 20 (1), 133-163.
- Patterson T. Treatment and prevention of fungal infections. Focus on candidemia. New York: Applied Clinical Education 2007, 23, 7-80.
- Levin M-D, den Hollander JG, van der Holt B, Rijnders B.J, Van Vliet M, Sonneveld P, van Schaik RH. Hepatotoxicity of oral and intravenous voriconazole in relation to cytochrome P450 polymorphisms. *Journal of Antimicrobial Chemotherapy* 2007, 60 (5), 1104-1107.
- Worth LJ, Blyth CC, Booth D, Kong DCM, Marriott D, Cassumbhoy M, Ray J, Slavin M, Wilkes J. Optimizing antifungal drug dosing and monitoring to avoid toxicity and improve outcomes in patients with haematological disorders. *Internal medicine journal* 2008, 38 (6b), 521-537.
- Fouda A, Hamza MF, Shaheen TI, Wei Y. Nanotechnology and smart textiles: Sustainable developments of applications. *Frontiers in Bioengineering and Biotechnology* 2022, 10, 1002887.
- Vinković Vrček, I., Selenium nanoparticles: Biomedical applications. *Selenium* 2018, 393-412.
- Ali M, Kim B, Belfield KD, Norman D, Brennan M, Ali GS. Green synthesis and characterization of silver nanoparticles using *Artemisia absinthium* aqueous extract—A comprehensive study. *Materials Science and Engineering: C* 2016, 58, 359-365.
- Procópio REdL, Silva IRd, Martins MK, Azevedo JLD, Araújo JMd. Antibiotics produced by *Streptomyces*. *Brazilian Journal of Infectious Diseases* 2012, 16, 466-471.
- Alani F, Moo-Young M, Anderson W. Biosynthesis of silver nanoparticles by a new strain of *Streptomyces* sp. compared with *Aspergillus fumigatus*. *World Journal of Microbiology and Biotechnology* 2012, 28, 1081-1086.
- Shaaban M, El-Mahdy AM. Biosynthesis of Ag, Se, and ZnO nanoparticles with antimicrobial activities against resistant pathogens using waste isolate *Streptomyces enissocaesilis*. *IET nanobiotechnology* 2018, 12 (6), 741-747.
- Jeffrey L. Isolation, characterization and identification of actinomycetes from agriculture soils at Semongok, Sarawak. *African Journal of Biotechnology* 2008, 7 (20).
- BL MP, Cole J, Lilburn T, Saxman P, Stredwick J, Garrity G, Li B, Olsen G, Pramanik S, Schmidt T. The RDP (ribosomal database project) continues. *Nucleic Acids Res.* 2000, 28, 173-174.
- Nikodinovic J, Barrow KD, Chuck J-A. High yield preparation of genomic DNA from *Streptomyces*. *Biotechniques* 2003, 35 (5), 932-936.
- Tamura K, Peterson D, Peterson N, Stecher G, Nei M, Kumar S. MEGA5: molecular evolutionary genetics analysis using maximum likelihood, evolutionary distance, and maximum parsimony methods. *Molecular biology and evolution* 2011, 28 (10), 2731-2739.
- Saitou N, Nei M. The neighbor-joining method: a new method for reconstructing phylogenetic trees. *Molecular biology and evolution* 1987, 4 (4), 406-425.

17. Shirling ET, Gottlieb D. Methods for characterization of *Streptomyces* species. *International journal of systematic bacteriology* 1966, 16 (3), 313-340.
18. Kumar V, Bharti A, Gusain O, Bisht GS. Scanning electron microscopy of *Streptomyces* without use of any chemical fixatives. *Scanning* 2011, 33 (6), 446-449.
19. Zonaro E, Lampis S, Turner RJ, Qazi SJS, Vallini G. Biogenic selenium and tellurium nanoparticles synthesized by environmental microbial isolates efficaciously inhibit bacterial planktonic cultures and biofilms. *Frontiers in microbiology* 2015, 6, 584.
20. Baygar T, Ugur A. Biosynthesis of silver nanoparticles by *Streptomyces griseorubens* isolated from soil and their antioxidant activity. *IET nanobiotechnology* 2017, 11 (3), 286-291.
21. Singh D, Rathod V, Fatima L, Kausar A, Vidyashree NA, Priyanka B. Biologically reduced silver nanoparticles from *Streptomyces* sp. VDP-5 and its antibacterial efficacy. *Int J Pharm Pharm Sci Res* 2014, 4 (2), 31-6.
22. Wayne P. Reference method for broth dilution antifungal susceptibility testing of yeasts, approved standard. CLSI document M27-A2 2002.
23. Makvandi P, Ghomi M, Padil VV, Shalchy F, Ashrafizadeh M, Askarinejad S, Pourreza N, Zarrabi A, Nazarzadeh Zare E, Kooti M. Biofabricated nanostructures and their composites in regenerative medicine. *ACS Applied Nano Materials* 2020, 3 (7), 6210-6238.
24. Roy A, Bulut O, Some S, Mandal AK, Yilmaz MD. Green synthesis of silver nanoparticles: biomolecule-nanoparticle organizations targeting antimicrobial activity. *RSC advances* 2019, 9 (5), 2673-2702.
25. Williams S, Cross T. Chapter XI actinomycetes. In *Methods in microbiology*, Elsevier: 1971; Vol. 4, pp 295-334.
26. Tan Y, Yao R, Wang R, Wang D, Wang G, Zheng S. Reduction of selenite to Se (0) nanoparticles by filamentous bacterium *Streptomyces* sp. ES2-5 isolated from a selenium mining soil. *Microbial cell factories* 2016, 15, 1-10.
27. Kumar V, Naik B, Gusain O, Bisht GS. An actinomycete isolate from solitary wasp mud nest having strong antibacterial activity and kills the *Candida* cells due to the shrinkage and the cytosolic loss. *Frontiers in Microbiology* 2014, 5.
28. Ikram M, Javed B, Raja NI, Mashwani Z-u-R. Biomedical potential of plant-based selenium nanoparticles: a comprehensive review on therapeutic and mechanistic aspects. *International Journal of Nanomedicine* 2021, 249-268.
29. Fesharaki PJ, Nazari P, Shakibaie M, Rezaie S, Banoe M, Abdollahi M, Shahverdi AR. Biosynthesis of selenium nanoparticles using *Klebsiella pneumoniae* and their recovery by a simple sterilization process. *Brazilian Journal of Microbiology* 2010, 41, 461-466.
30. Zhang W, Chen Z, Liu H, Zhang L, Gao P, Li D. Biosynthesis and structural characteristics of selenium nanoparticles by *Pseudomonas alcaliphila*. *Colloids and Surfaces B: Biointerfaces* 2011, 88 (1), 196-201.
31. Hassan MG, Hawwa MT, Baraka DM, El-Shora HM, Hamed AA. Biogenic selenium nanoparticles and selenium/chitosan-Nanoconjugate biosynthesized by *Streptomyces parvulus* MAR4 with antimicrobial and anticancer potential. *BMC microbiology* 2024, 24 (1), 21.
32. Dhanjal S, Cameotra SS. Aerobic biogenesis of selenium nanospheres by *Bacillus cereus* isolated from coalmine soil. *Microbial cell factories* 2010, 9 (1), 1-11.
33. Kora AJ, Rastogi L. Biomimetic synthesis of selenium nanoparticles by *Pseudomonas aeruginosa* ATCC 27853: an approach for conversion of selenite. *Journal of environmental management* 2016, 181, 231-236.
34. Hashem AH, Saied E, Amin BH, Alotibi FO, Al-Askar AA, Arishi AA, Elkady FM, Elbahnasawy MA. Antifungal activity of biosynthesized silver nanoparticles (AgNPs) against aspergilli causing aspergillosis: Ultrastructure Study. *Journal of Functional Biomaterials* 2022, 13 (4), 242.
35. Ramya S, Shanmugasundaram T, Balagurunathan R. Biomedical potential of actinobacterially synthesized selenium nanoparticles with special reference to anti-biofilm, anti-oxidant, wound healing, cytotoxic and anti-viral activities. *Journal of Trace Elements in Medicine and Biology* 2015, 32, 30-39.
36. Saied E, Eid AM, Hassan SE-D, Salem SS, Radwan AA, Halawa M, Saleh FM, Saad HA, Saied EM, Fouda A. The catalytic activity of biosynthesized magnesium oxide nanoparticles (MgO-NPs) for inhibiting the growth of pathogenic microbes, tanning effluent treatment, and chromium ion removal. *Catalysts* 2021, 11 (7), 821.
37. Chi NTL, Veeraragavan GR, Brindhadevi K, Chinnathambi A, Salmen SH, Alharbi SA, Krishnan R, Pugazhendhi A. Fungi fabrication, characterization, and anticancer activity of silver nanoparticles using metals resistant *Aspergillus niger*. *Environmental Research* 2022, 208, 112721.

38. Lazcano-Ramírez HG, Garza-García JJ, Hernández-Díaz JA, León-Morales JM, Macías-Sandoval AS, García-Morales S. Antifungal Activity of Selenium Nanoparticles Obtained by Plant-Mediated Synthesis. *Antibiotics* 2023, 12 (1), 115.
39. Chudobova D, Cihalova K, Dostalova S, Ruttkay-Nedecky B, Merlos Rodrigo MA, Tmejova K, Kopel P, Nejdil L, Kudr J, Gumulec J. Comparison of the effects of silver phosphate and selenium nanoparticles on *Staphylococcus aureus* growth reveals potential for selenium particles to prevent infection. *FEMS microbiology letters* 2014, 351 (2), 195-201.
40. Xu X, Cheng J, Zhou Y, Zhang C, Ou X, Su W, Zhao J, Zhu G. Synthesis and antifungal activities of trichodermin derivatives as fungicides on rice. *Chemistry & Biodiversity* 2013, 10 (4), 600-611.
41. Truong LB, Medina-Cruz D, Mostafavi E, Rabiee N. Selenium nanomaterials to combat antimicrobial resistance. *Molecules* 2021, 26 (12), 3611.